ARTICLE

Check for updates

Developmental exposure to non-dioxin-like polychlorinated biphenyls promotes sensory deficits and disrupts dopaminergic and GABAergic signaling in zebrafish

Nadja R. Brun [1✉], Jennifer M. Panlilio [1], Kun Zhang[2,3], Yanbin Zhao[2,3], Evgeny Ivashkin[4,5], John J. Stegeman [1,6✉] & Jared V. Goldstone [1,6✉]

The most abundant polychlorinated biphenyl (PCB) congeners found in the environment and in humans are neurotoxic. This is of particular concern for early life stages because the exposure of the more vulnerable developing nervous system to neurotoxic chemicals can result in neurobehavioral disorders. In this study, we uncover currently unknown links between PCB target mechanisms and neurobehavioral deficits using zebrafish as a vertebrate model. We investigated the effects of the abundant non-dioxin-like (NDL) congener PCB153 on neuronal morphology and synaptic transmission linked to the proper execution of a sensorimotor response. Zebrafish that were exposed during development to concentrations similar to those found in human cord blood and PCB contaminated sites showed a delay in startle response. Morphological and biochemical data demonstrate that even though PCB153-induced swelling of afferent sensory neurons, the disruption of dopaminergic and GABAergic signaling appears to contribute to PCB-induced motor deficits. A similar delay was observed for other NDL congeners but not for the potent dioxin-like congener PCB126. The effects on important and broadly conserved signaling mechanisms in vertebrates suggest that NDL PCBs may contribute to neurodevelopmental abnormalities in humans and increased selection pressures in vertebrate wildlife.

[1] Department of Biology, Woods Hole Oceanographic Institution, Woods Hole, MA, USA. [2] School of Environmental Science and Engineering, Shanghai Jiao Tong University, 800 Dongchuan Road, Shanghai 200240, China. [3] Shanghai Institute of Pollution Control and Ecological Security, Shanghai 200092, China. [4] Josephine Bay Paul Center for Comparative Molecular Biology and Evolution, Marine Biological Laboratory, Woods Hole, MA, USA. [5] A.N. Severtsov Institute of Ecology and Evolution, Russian Academy of Sciences, Moscow, Russia. [6] These authors jointly supervised this work: John J. Stegeman, Jared V. Goldstone. ✉email: nbrun@whoi.edu; jstegeman@whoi.edu; jgoldstone@whoi.edu

Humans and wildlife are exposed to a wide range of contaminants in the environment and the role of these chemical pollutants in developmental neurotoxicity and neurodegenerative disorders has become a global environmental health concern[1]. Among the top industrial-derived contaminants thought to be involved in developmental neurotoxicity are polychlorinated biphenyls (PCBs)[2–4]. For decades, PCBs have been used as insulators, coatings, and caulks, and have persisted to date in the environment where they have globally accumulated in wildlife tissue and human cord blood, amniotic fluid, and mother's milk[5,6]. PCBs are a group of organochlorine compounds comprised of 209 structurally similar analogues, or congeners. They are often subdivided into congeners that share a structural and toxicological similarity with dioxins, the dioxin-like (DL) PCBs and non-dioxin-like (NDL) PCBs. The levels of NDL PCBs in human and environmental samples are far greater than the levels of DL congeners, with NDL PCB153 and PCB138 being the most abundant. In human cord blood, PCB153 concentrations range from 3.7 to 200 ng g^{-1} lipid (10–554 nM)[7–10].

During the early stages of life, the nervous system is generally more sensitive to chemical exposure compared to fully developed adults[11], and, therefore, it is essential to identify the neurotoxic mechanisms that underpin the behavioral effects of environmental exposure to different PCBs during gestation and early life stages if we want to successfully treat and remediate health effects in humans and wildlife. Early developmental exposure to PCBs is associated with many neurodevelopmental disorders. For instance, increased serum PCB concentrations in children are associated with deficits in cochlear functions[12,13], fine motor skills[14,15], and cognitive impairment[4,16]. In rats, developmental exposure to NDL PCBs has been linked to behavioral changes, including hyperactivity, impulsiveness, and impairment of cognitive function[3,17,18]. NDL PCB developmental exposure also adversely affect the auditory function in adult rats, including elevated thresholds of brainstem auditory evoked potentials, auditory deficits at low frequencies, audiogenic seizures, and reduced auditory startle responses[19–23]. The observed effect on the auditory-evoked startle response is particularly relevant as it plays a critical role in the performance and survival of fish and amphibians, and involves cellular functions, sensory-motor pathways, and monoamine neurotransmitters that, ranging from fish to humans, are conserved among vertebrates[24].

To date, mechanistic studies of neurodevelopmental effects of NDL PCBs suggest three major targets: (1) alterations in neurotransmission, particularly involving dopamine and serotonin, and consequently disruptions to Ca^{2+} signal transduction[25–29], (2) loss of outer hair cells[12,19], and (3) altered axonal or dendritic morphogenesis[30–33]. The links between these PCB targets and neurobehavioral deficits remain unknown.

We used the zebrafish auditory system as a model to decipher the involvement of these three major targets in disrupting the startle response after developmental exposure to NDL PCB153. Many of the pathways and genes that regulate startle behavior in fish also operate in human neurological disorders[34–38]. We demonstrate that environmentally relevant concentrations (10 nM) of NDL PCB153 alter startle response which coincided with axonal swelling and dysregulated dopamine metabolite and GABA levels. Co-exposures to the dopamine D2-receptor antagonist and GABA receptor modulator drug haloperidol alleviated the delay in startle response. While similar responses were observed for other di-*ortho* NDL PCBs and the mono-*ortho* congener PCB118, a delayed startle response was not observed with the non-*ortho* PCB126, a potent AHR agonist. These results highlight the potential of low concentrations of NDL PCBs to disrupt broadly conserved neurotransmission tied to a mechanosensory deficit.

Results

Morphological effects. Exposure to contaminants during development can result in reduced growth, which can affect kinematics in swimming behavior[39]. Zebrafish larvae exposed to 1000 nM PCB153 developed normally with no difference in body length at 6 dpf in comparison to the control group, in three separate trials (Trial 1: $t(25.98) = 0.661$, $p = 0.5144$; Trial 2: $t(37.98) = 0.443$, $p = 0.6604$; Trial 3: $t(37.43) = 0.645$, $p = 0.5232$; Supplementary Fig. 1).

Behavioral effects. Rohon-Beard cells are mechanosensory neurons that appear earliest during development in zebrafish. They are located in the dorsal region of the embryonic spinal cord and appear around 24 h post-fertilization (hpf)[40]. A few days into development, Rohon-Beard cells also relay sensory information to the Mauthner cells[41]. In our experiments, a tactile stimulus on the trunk at 26 hpf evoked a C-shaped body flexion in both the DMSO- and the 1000 nM PCB153-treated embryos ($U = 183$, $p = 0.5989$; Supplementary Fig. 2), indicating that the formation and function of Rohon-Beard cells were not impaired by PCB153.

Spontaneous and light–dark-stimulated swimming activity assessed at 6 dpf revealed that larvae exposed to PCB153 (1000 nM) had lower cumulative locomotion activity over ten minutes ($M = 1182$ mm, $SD = 382$) in comparison to the control group ($M = 1510$ mm, $SD = 402$), $t(132.4) = 4.854$, $p < 0.0001$ (Supplementary Fig. 3a). Zebrafish larvae typically increase locomotion in dark conditions following light exposure. Once stimulated by a rapid loss of illumination, both treatment groups exhibited similar swimming activity (Supplementary Fig. 3b), indicating the capability of visual response and fast movements in the treated larvae.

The neural circuit underlying the vibro-acoustic startle response in fish transmits excitatory input from multisensory afferents, to the Mauthner cells that project to the motor neurons (Fig. 1). The resulting behavioral response includes two distinct motor behaviors: a short-latency C-bend (SLC) initiated within 5–15 ms of the stimulus, or a long-latency C-bend (LLC) beginning from 15–100 ms after the stimulus[42]. The mean latency value calculated as the average of all SLC and LLC responses in each treatment population was 21 ± 20 ms for control larvae at the highest vibro-acoustic stimulus intensity (Fig. 2a, b). By contrast, the NDL PCB-treated larvae that responded to the stimulus showed significantly longer average latencies in response to the same stimulus intensity given the controls, $H(8) = 368.6$, $p < 0.0001$ (Fig. 2b; Supplementary Movie 1, for legend see the description of additional Supplementary Information). Larvae exposed to PCB153 responded at mean latencies that increased with dose. Thus at 10 nM PCB153 the latency was 26 ± 27 ms, at 30 nM it was 50 ± 36 ms, at 100 nM it was 50 ± 30 ms, and at 1000 nM the latency was 68 ± 32 ms. Results with the lowest PCB153 concentration tested (10 nM) were not significantly different from controls ($p = 0.7521$). Larvae exposed to other NDL congeners also showed long latencies; with PCB138 it was 52 ± 37 ms, with PCB118 it was 45 ± 27 ms, and with PCB52 it was 39 ± 32 ms. Unlike the NDL PCB-treated larvae, larvae treated with the potent DL PCB126 had a mean latency of 22 ± 22 ms, essentially identical to that in the controls ($p = 0.9999$).

Examining the SLC and the LLC responses separately can give insight into the underlying mechanism of effect. A greater stimulus intensity increases the probability of evoking an SLC, shifting the response bias from LLC to SLC[43]. Consistent with that we observed a shift to SLC with increasing stimulus intensity in solvent control (DMSO-treated) larvae (Fig. 2c). Larvae were tested 4 times at each stimulus intensity. A larva is categorized as
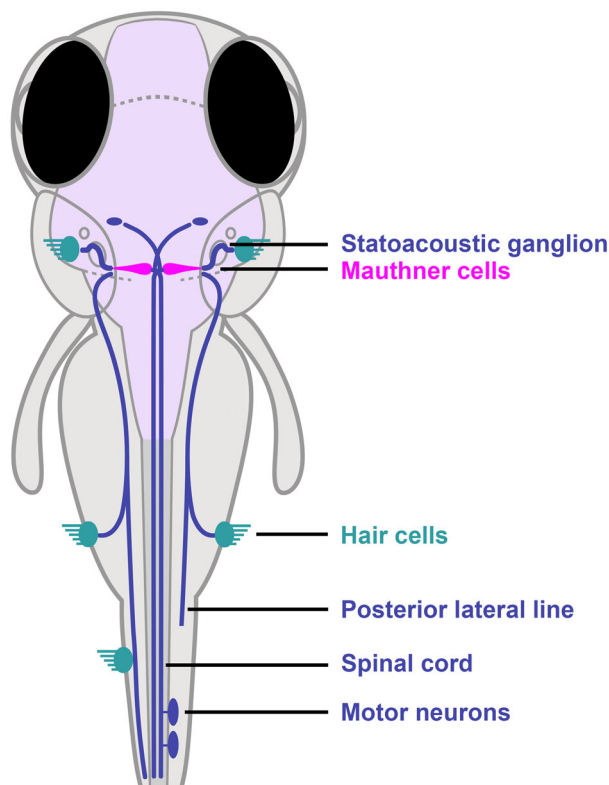
Fig. 1 Startle response circuit in zebrafish. The proper execution of the auditory-evoked startle response relies on hair cells to sense the auditory stimulus, Mauthner cells to integrate the signals, and motor neurons and musculature to execute the startle behavior.

having SLC bias if it responded with an SLC 3 or 4 times out of the 4 tests. At the highest stimulus intensity that we tested (43 dB), the majority of control larvae (300/448) responded with an SLC within 7 ± 3 ms. There were 43 larvae that showed no bias towards SLC or LLC (2 times SLC and 2 times LLC, bias = 0). There also were larvae that did not perform an SLC ($n = 105$) but did exhibit an LLC, with a mean latency of 54 ± 29 ms (Fig. 2c). In contrast, all NDL PCB-treated larvae retained a response bias towards LLC at all stimulus intensities tested, which was significantly different from the control (GLM, $p < 0.01$ for the three highest stimulus intensities; for exact p-values see Supplementary Table 1; Fig. 2c). As we decreased the PCB153 dose, there was an increased shift towards an SLC, yet even at 10 nM PCB153 the bias toward LLC was significantly different from the control (GLM, $p < 0.01$ for all stimulus intensities, Fig. 2c). PCB153 exposures starting at 24 hpf, after many structures of the brain and the neural tube have developed[44], had the same effect on startle latency as exposures starting at 4 hpf (Supplementary Fig. 4b), suggesting that the mechanism leading to the startle latency is initiated after the major neuronal structures are developed. It would be informative to see if any morphological changes at 6 dpf would occur in larvae exposed from 4 to 24 hpf.

The proportion of control larvae responding to the stimulus (with either an SLC or an LLC) increased from $75.2 \pm 33.0\%$ ($n = 450$) to $95.8 \pm 17.0\%$ ($n = 457$) from the lowest to highest stimulus intensity (Fig. 2d). In contrast, the proportion of PCB153-, PCB138-, and PCB52-treated larvae that responded remained below 70% at all intensities and were significantly different ($p < 0.01$; for exact p-values see Supplementary Table 1) from the control, except for the larvae exposed to 10 nM PCB153 (Fig. 2d, Supplementary Fig. 5a). The larvae exposed to the DL

PCB126 and NDL PCB118 had a response latency and rate similar to the control larvae.

The kinematics of the C-bend angle differ for the SLC and LLC startle responses, with SLCs exhibiting larger bend angles and faster angular velocities than LLCs[42]. For each PCB, we examined the bend angles separately in SLC and LLC. Generally, there were increased bend angles associated with SLC response after NDL PCB exposure, even when there were very few SLC responders. Similarly, there were generally decreased bend angles in the LLC responders after NDL PCB exposures (Supplementary Fig. 6).

Cellular structures. The execution of the startle response is mediated by hair cells that sense the auditory stimulus, Mauthner cells that integrate the signals, and motor neurons and musculature that execute the startle behavior (Fig. 1). Imaging of Mauthner cells, motor neurons, and musculature showed that all appeared to be present in PCB153 exposed larvae, but the neurons innervating the hair cells appeared to be swollen (Fig. 3). The L3 neuromast volume of control larvae was on average 569 μm^3 ($SD = 125$), whereas larvae exposed to PCB153 (1000 nM) had significantly larger L3 neuromast volumes 848 μm^3 ($SD = 185$), $t(48.93) = 6.765$, $p < 0.0001$ (Fig. 3b). However, the number of hair cells in L3 neuromasts remained unchanged (Fig. 3c). The hair cells also appeared to be functional in PCB153-treated and control larvae as shown by equal internalization of the fluorescent dye FM1-43 (n-(3-triethylammoniumpropyl)-4-(4-(dibutylamino)-styryl) pyridinium dibromide) (Fig. 3d), a dye that specifically labels hair cells in the lateral line and inner ear of vertebrates by entering through open mechanotransduction channels and filling the cytoplasm of hair cells[45].

The presence of functional Mauthner cells is necessary for the SLC startle response. Staining with monoclonal antibody 3A10 confirmed the presence of Mauthner cells in all PCB153-exposed larvae (21/21) (Fig. 4a). We tested the functional responsiveness of the Mauthner cells by applying electric field pulses to head-restrained larvae. This electrical stimulation (Fig. 4b) bypasses the sensory system and directly activates the Mauthner cell[46]. There was no difference detected in response time between control and 1000 nM PCB153-exposed larvae ($U = 907.5$, $p = 0.4892$), demonstrating that the signal transmission from the Mauthner cell to the motor neurons is not disrupted in the PCB153-exposed fish (Fig. 4c). The fraction responding also was similar in both the DMSO-treated (290/299) and the PCB153-treated (209/219) groups (GLM, $p = 0.427$; Fig. 4d). However, the angle of the C-bend evoked by the electrical stimulation was larger in PCB153-exposed larvae ($M = 101.4$, $SD = 38.60$) than in the control larvae ($M = 83.12$, $SD = 24.23$). An unpaired t-test with Welch's correction indicated that this difference was statistically significant, $t(74.27) = 2.679$, $p = 0.0091$ (Fig. 4e). This difference could indicate a PCB153-evoked sub-cellular alteration of the Mauthner cell axon or the motor neuron.

For rapid and effective axonal signal transmission, proper myelination of axons is key. We did not find PCB153 to reduce cells of the oligodendrocyte lineage in the spinal cord of the *Tg(olig2:EGFP)* transgenic line treated with PCB153, ($t(36) = 0.553$, $p = 0.5839$). We also did not find any differences in myelination itself in the *Tg(mbp:EGFP-CAAX)* transgenic line treated with PCB153 (Supplementary Fig. 7).

Proper function and activation of the motor neurons are crucial for the completion of the startle circuit, leading to muscle contractions and the characteristic swimming behaviors. The main caudal primary (CaP), middle primary (MiP), and rostral primary (RoP) motor neurons did not show any distinct structural differences between exposed and control larvae (Supplementary Fig. 8). The fast muscle fibers in the myotome were not differentially striated in the PCB153 treatment group
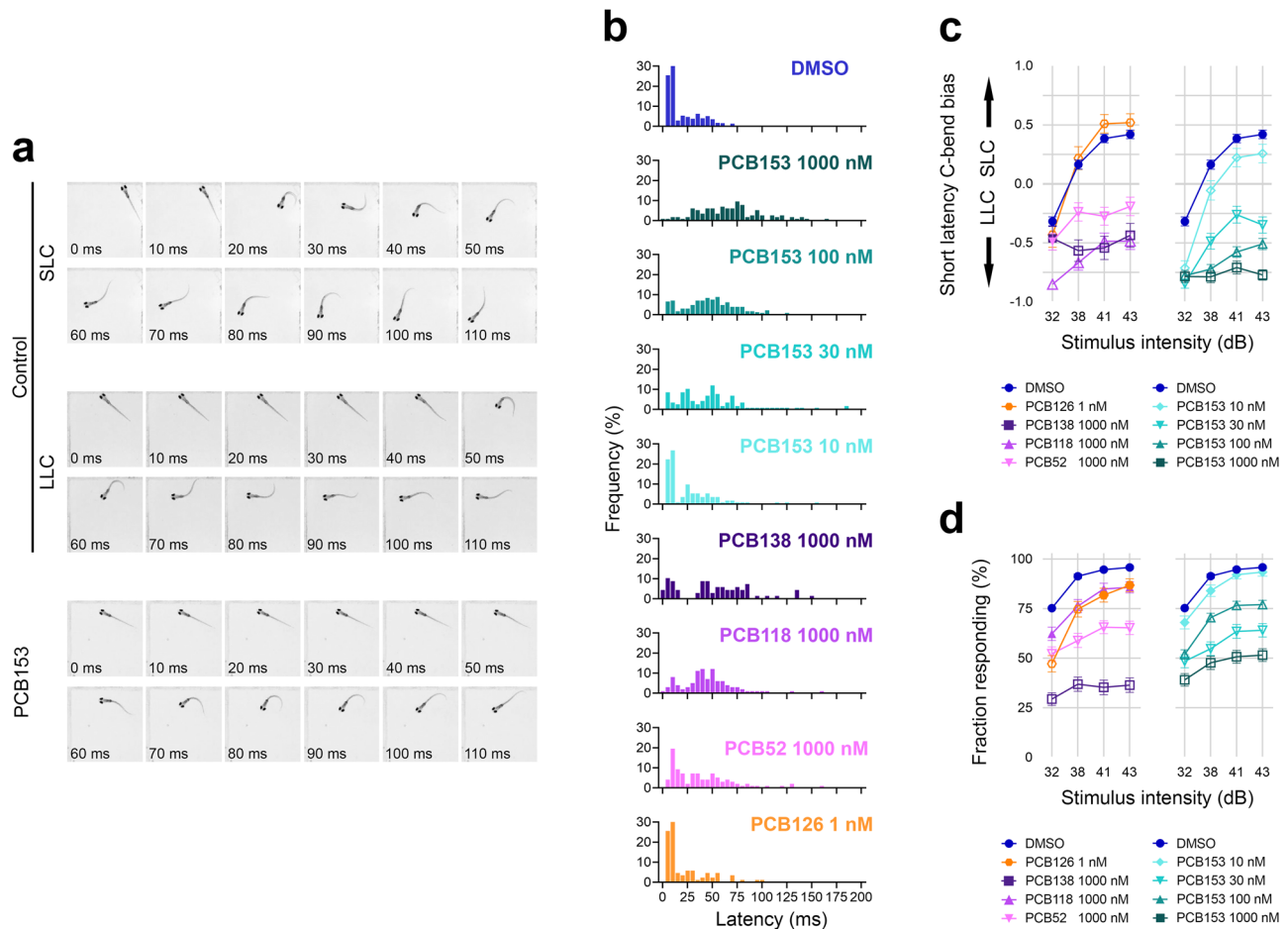
Fig. 2 Effect of PCBs on startle response in 6 dpf zebrafish. a Representative short-latency C-bend (SLC) and long-latency C-bend (LLC) startle response of a control zebrafish larva at 6 dpf in comparison to a typical response of a PCB153 treated larva. **b** Vibro-acoustic startle latency at highest stimulus intensity (43 dB) in vehicle control ($n = 448$), NDL PCB153 1000 nM ($n = 115$), NDL PCB153 100 nM ($n = 226$), NDL PCB153 30 nM ($n = 117$), NDL PCB153 10 nM ($n = 112$), NDL PCB138 ($n = 68$), NDL PCB118 ($n = 99$), NDL PCB52 ($n = 97$), and DL PCB126 ($n = 86$) exposed larvae. **c** Bias of SLC and LLC and **d** response rate of different exposure groups at different vibro-acoustic intensities. All data points are biologically independent samples from at least three independent experiments and mean ± SEM shown in the plots of (**c**, **d**). Binomial GLM was used for statistical analysis in (**c**, **d**). Significant differences to DMSO controls ($p < 0.01$) are indicated by open symbols.

(Supplementary Fig. 9). No structural difference in the motor neurons or the myotome was apparent in PCB153-exposed larvae, suggesting that the increased bend angle does not originate from any overt structural differences in the motor neurons or muscle fibers.

Neuronal activity. The release of neurotransmitters into the synaptic cleft is a characteristic process in signal transmission. Both serotonergic and dopaminergic neuromodulators can affect startle latency[47], and evidence has been found that NDL PCBs alter these neuromodulators in mammals (e.g., Mariussen & Fonnum[48]; Enayah et al.[28]; Wigestrand et al.[49]). We observed that PCB153 (1000 nM) altered the levels of several neurotransmitters in 6 dpf zebrafish larvae (Fig. 5a). Significantly increased levels of GABA ($t(6) = 9.719$, $p < 0.0001$), a main precursor of acetylcholine (choline-chloride; $t(6) = 8.459$, $p = 0.0002$), a major dopamine metabolite (3-methoxytyramine hydrochloride; $t(6) = 3.803$, $p = 0.0089$), and an amino acid involved in the synthesis of serotonin (L-valine; $t(6) = 3.134$, $p = 0.0202$) were measured in PCB-exposed larvae in comparison to control larvae, while L-glutamine, a precursor to both the excitatory neurotransmitter glutamate and inhibitory neurotransmitter GABA,

was decreased in comparison to control larvae ($t(6) = 5.966$, $p = 0.0010$).

To assess the interaction between PCB exposure and changes in neuromodulatory activity, we pharmacologically manipulated the neurotransmitter levels using serotonin, dopamine, and GABA receptor agonists, antagonists, and precursors. In control larvae, a 30 min exposure to serotonin precursor 5-HTP, dopamine precursor L-DOPA ($p < 0.01$; for exact p-values see Supplementary Table 1; Fig. 5b) and D2-receptor agonist quinpirole ($p < 0.01$; Supplementary Fig. 4d) shifted the response to LLC, at multiple intensities tested. In contrast, the dopamine antagonist haloperidol exposure induced a shift to SLC in controls across all four stimulus intensities ($p < 0.01$; Fig. 5b). Haloperidol induced the same shift to SLC in PCB153-exposed larvae ($p < 0.001$), suggesting that the startle circuit is functional but repressed by PCB153 (Fig. 5b). The antagonist to the $GABA_A$ receptor, bicuculline, did not affect the SLC response bias, either in the control or in the PCB153-exposed larvae, except for the highest stimulus intensity in the control (Fig. 5b). The response rate remained unchanged after exposure to neurotransmitter modulators except for 5-HT, which caused an increase in response probability across all stimulus intensities in control
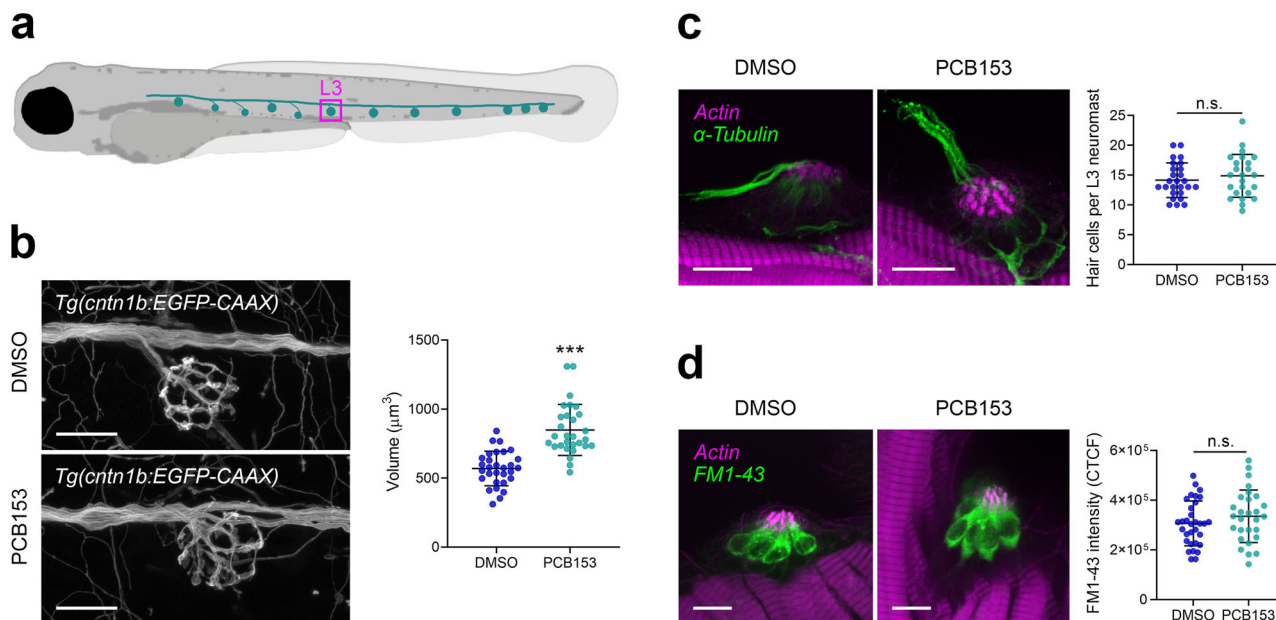
Fig. 3 Effect of PCB153 on morphology and function of lateral line hair cells and innervating neurons. a Diagram indicating L3 neuromast. **b** Hair cell innervating neurons at neuromast L3 shown using *Tg(cntn1b:EGFP-CAAX)* and volume of hair cell innervating neurons of DMSO ($n = 30$) and PCB153 ($n = 29$) treated larvae. Scale bar = 20 μm. **c** Whole-mount immunostaining of kinocilia and hair cell innervating neurons (anti-acetylated tubulin antibody; green) and counterstain of stereocilia bundles and muscle tissue (actin; magenta) of DMSO ($n = 26$) and PCB153 ($n = 24$) treated larvae. The hair cell number was determined based on the number of kinocilia. Scale bar = 10 μm. **d** Uptake of FM1-43 dye as indication of functional hair cells of DMSO ($n = 32$) and PCB153 ($n = 28$) treated larvae. CTCF = Corrected total cell fluorescence. Scale bar = 10 μm. All data points are biologically independent samples from three independent experiments and mean ± SD are shown in the plots. Unpaired two-tailed *t*-test with Welch's correction was used for statistical analysis in (**b**, **c**), a two-way ANOVA accounting for trial and treatment in (**d**). Asterisks indicate significant differences to controls (***$p < 0.001$).

larvae ($p < 0.01$); quinpirole, which caused a decrease in response probability at the two lowest stimulus intensities in control larvae ($p < 0.01$); and haloperidol, which caused an increase in response probability at 41 dB in PCB153-treated larvae ($p < 0.01$; Supplementary Fig. 5). It is noteworthy, that co-exposure to L-DOPA and PCB153 throughout development increased the startle response rate of PCB153-treated larvae significantly ($p < 0.01$; Supplementary Fig. 5c), yet only induced a significant shift towards SLC at 38 dB ($p < 0.01$; Supplementary Fig. 4c).

In the fish brain, a distinct population of serotonergic neurons is found in the posterior tuberculum/hypothalamus, forming a prominent horseshoe-like pattern that is one of several brain regions where 5-HT is synthesized[50]. To assess whether the neuroanatomical organization or neurogenesis of serotonergic cells in the hypothalamus of PCB153 larvae was affected, we performed immunohistochemistry using an antibody for 5-HT (Supplementary Fig. 10). The intensity of the fluorescent signal in the hypothalamus was not different, comparing PCB153 ($M = 4.70 \times 10^6$, $SD = 2.10 \times 10^6$) with the control ($M = 4.38 \times 10^6$, $SD = 8.1 \times 10^5$) group. This suggests that the serotonergic neurons in this region were not affected.

During specific behaviors or sensory experiences, only a small percentage of neurons are active. We examined the active neuronal cell populations in PCB153-treated and -untreated larvae, focusing on the rostral hindbrain where the Mauthner cells are located. To assess whether there were changes in neuronal activity, we used the CaMPARI zebrafish line, which contains a protein that upon UV illumination permanently photoconverts from green to red fluorescence in cells with high calcium levels[51]. This genomic tool enabled us to look for active neuronal cell populations in larvae during normal swimming movement and in larvae experiencing a vibroacoustic-stimulated startle response. At room temperature (24 °C) no difference in the red to green ratio (F_{red}/F_{green}) was measured comparing control

and PCB153-treated larvae, either when swimming or startling (Supplementary Fig. 11). However, when stimulating high calcium turnover by placing the larvae in cold (4 °C) medium, swimming control larvae exhibited higher F_{red}/F_{green} ratio ($M = 2.30$, $SD = 0.51$) in comparison to swimming PCB153-treated larvae ($M = 1.70$, $SD = 0.31$) on average across two trials (Fig. 5c). Importantly, the difference between control and PCB153-treated larvae swimming in cold medium was significant in both trials (trial 1: $F(1, 18) = 121$, *adj.* $p = 0.0277$ and trial 2: $F(1, 32) = 65.2$, *adj.* $p = 0.0004$). Similar differences in neuronal activity between control and PCB153 treated larvae were measured for startling larvae (Supplementary Fig. 11).

Discussion

While their use has mostly ended decades ago, PCBs remain a globally important and persistent group of pollutants that continues to impact both wildlife and humans. Prenatal exposure to PCBs is now recognized to contribute to neurobehavioral disorders in humans and potentially other organisms, yet the mechanisms that underlie this neurotoxicity remain largely unknown[52]. Using developmental exposure of zebrafish to PCB153, we identify here an imbalance in dopamine metabolites and GABA mediating mechanosensory deficits, encompassing hearing and touch in fish. The behavioral effect was found to be specific to NDL PCBs and at concentrations relevant for both humans and aquatic life. These findings highlight a so far unrecognized impact of commonly observed concentrations of NDL PCBs on the escape response in fish and link a conserved neurotoxic mechanism to behavioral deficits.

We observed a delayed startle response for all NDL PCBs tested and subsequently examined a number of cellular features of the underlying startle circuit anatomy (hair cell, afferent neurons, Mauthner cell, oligodendrocyte lineage cells, myelination, motor
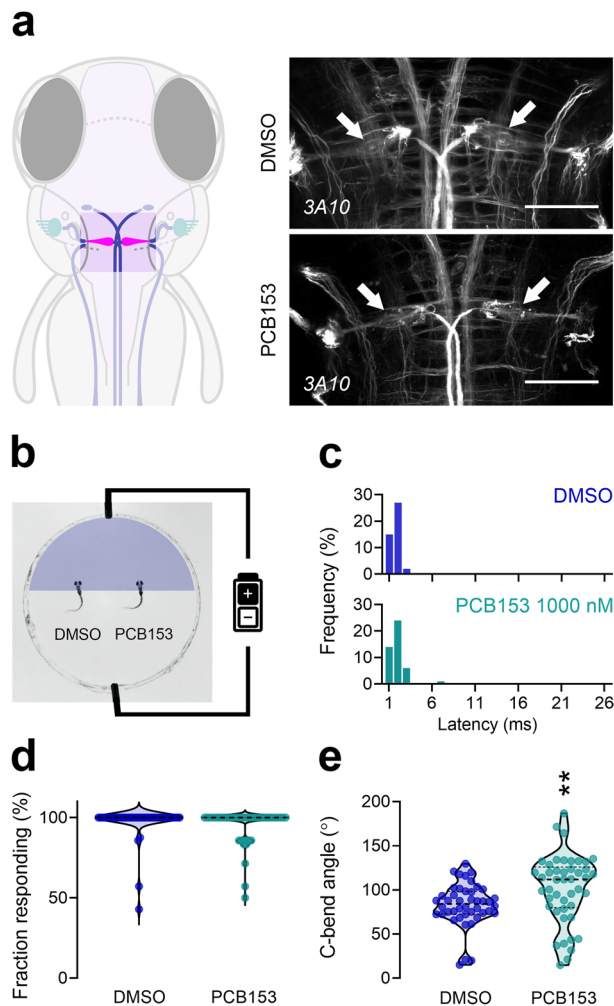
Fig. 4 Effect of PCB153 on presence and function of the Mauthner cells. **a** Diagram indicating localization of Mauthner cells in the hindbrain and brain tissue immunostaining with anti-neurofilament 3A10 antibody labeling reticulospinal neurons in control and PCB153 treated larvae at 6 dpf (ventral view). Mauthner (arrow) cells were present in all brain tissues (DMSO: $n = 23$, PCB153: $n = 21$, biologically independent samples). Scale bar = 50 μm. **b** Diagram of electrical stimulation performed to assess the functionality of Mauthner cells. Both DMSO ($n = 44$) and PCB153 ($n = 45$) treated larvae show similar **c** latency to electrical stimulation and **d** response frequency, indicating that the Mauthner cells are present and functional, **e** while the C-bend angle in PCB153 exposed larvae was increased (Welch's t-test, $**p = 0.0091$). All data points are biologically independent samples (one value representing the mean of seven consecutive electric field pulses) from three independent experiments and mean ± SD are shown in the plots. Mann–Whitney test was used for statistical analysis in (**c**), binomial GLM in (**d**), and unpaired two-tailed t-test with Welch's correction in (**e**). Dashed lines represent median and quartiles and asterisks indicate significant differences to controls.

neuron, muscle; Fig. 1), as potentially affected by the NDL PCB153. Only the volume of the neurons that innervate the hair cells showed a measurable deviation from the control condition in PCB153-exposed larvae (Fig. 3). We thus infer that the enlargement of axon termini is contributing to the neurotoxic potential of NDL PCBs. This is an understudied target of PCB toxicity with only a few studies associating NDL PCB exposure with altered dendritic arborization[32,33,52]. The direct links to neurobehavioral changes remain to be shown. However, swelling of afferent terminals is associated with hearing deficits in both mammalian

models (Puel et al.[53]) and zebrafish (Sebe et al.[54]). Axonal swelling is also a pathology appearing in many neurodegenerative diseases[55], thus exposure to NDL PCBs may be a contributing factor in such diseases.

The proper function of the Mauthner cell is essential in transmitting the signal that leads to the rapid startle response. At the structural level, laser-ablation of the Mauthner cell abolishes SLC responses without affecting LLC responses[56]. Our finding that NDL PCB-exposed larvae predominantly exhibit LLC without loss of Mauthner cells (Figs. 2c, 4a), suggests that the Mauthner cells are receiving a delayed input, are not firing properly, or that the signal propagation downstream of the Mauthner cell is disrupted. To distinguish these, we directly activated the Mauthner cells by applying electrical stimulation to larvae with their heads restrained and found that, unlike auditory stimulation, PCB153-exposed fish had latencies indistinguishable from the controls (Fig. 4c). Furthermore, direct electrical stimulation of PCB153-exposed larvae resulted in a normal response rate (Fig. 4d), although the bend angle was substantially increased (Fig. 4e). These results indicate a proper function of Mauthner cells in NDL PCB-treated larvae. However, the changes in bend angles we observed during these responses could indicate alterations downstream of the Mauthner cells.

Little is known about the mechanisms leading to a distorted turning angle. Since we found no obvious structural impairment downstream of the Mauthner cell (oligodendrocyte lineage cells, myelination, motor neuron, musculature), we speculate that the increased bend angle in electrically stimulated larvae exposed to PCB153 may be linked to a sub-cellular disruption such as gap junctions. Gap junctions are specialized intercellular connection known to link the Mauthner cells to their sensory afferents, and, if affected, one would expect an increased bend-angle in response to electrical stimulation as well as in response to sensory stimulation. This is the case for electrical stimulation as well as the highest stimulus intensity of the auditory stimulation, where a reasonable number of larvae ($n = 26$) respond with an SLC (Supplementary Fig. 6). It is known that PCBs can alter gap junction function in cells of many organs[57–59] including NDL PCB specific inhibition of gap junctional intercellular communication in neural crest cells[60] and neuronal stem cells[61]. Gap junctions are intercellular channels formed by connexins (Cx). RNA sequencing of zebrafish larvae exposed to PCB153 in a similar exposure regime (4-120 hpf) and concentration (10 μM) substantially altered the expression of connexin genes $cx28.9$, $cx42$, and $cx35b$[62,63]. $cx35$ is expressed on the Mauthner neuron lateral dendrites in zebrafish[47] and plays a crucial role in regulating spinal motor activity during fast motor behavior of adult mosquitofish[64]. We thus suggest that gap junction function could be disrupted, which may be a future study direction.

Neurotransmitters are key to startle responses, provided that more than 1000 pharmacologically active compounds are identified serotonergic and dopaminergic modulators among the largest class of drugs that shift bias between SLC and LLC startle behavior[47]. Specifically, acute exposure to the D3R agonist (7OHD) shifts the startle bias from LLC to SLC, while exposure to a D3R antagonist (or a 5-HT1AR agonist) shifts bias toward LLC behavior[47]. Our results extend these findings, showing that 30 min of exposure to L-DOPA or 5-HTP induced a shift from SLC to LLC at higher stimulus intensities, as opposed to the D2R antagonist haloperidol, which evoked a shift to a stronger SLC bias at all stimulus intensities (Fig. 5b). NDL PCBs are thought to affect dopaminergic pathways[49,65], which is partly supported by our measurements of catecholamines and traces amines. Specifically, we found that the extracellular dopamine metabolite
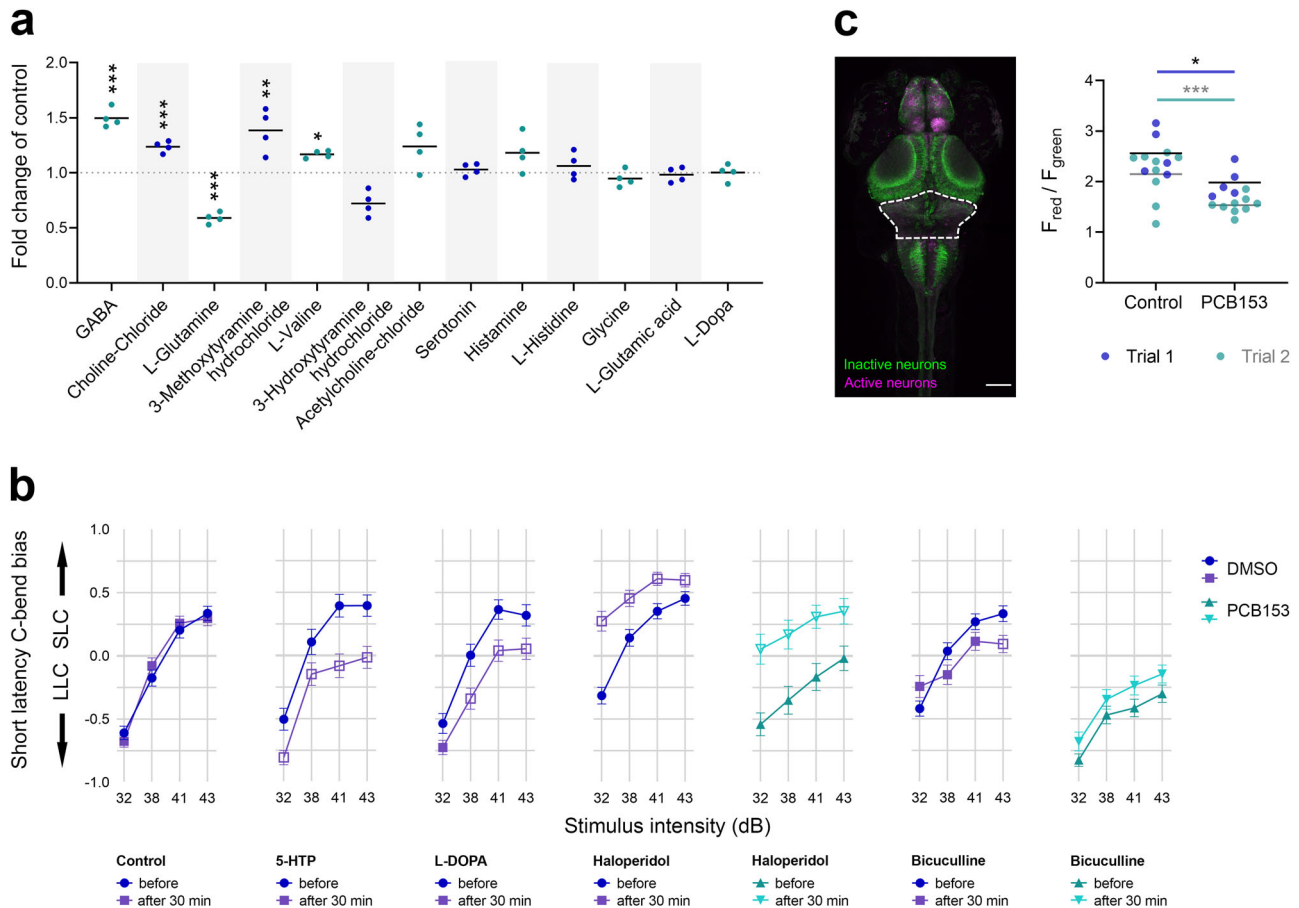
Fig. 5 Involvement of neurotransmitters in startle latency. a Neurotransmitter levels in 6 dpf larvae exposed to 1000 nM PCB153 in comparison to control ($n = 4$, pool of 18 larvae per sample). Unpaired t-test GABA ***$p = 0.00007$, choline-chloride ***$p = 0.0001$, L-glutamine ***$p = 0.0010$, 3-methoxytyramine hydrochloride **$p = 0.0089$, L-valine *$p = 0.0202$. **b** Startle bias shift induced by 30-min exposure to serotonin, dopamine, and GABA neurotransmitter modulators in 6 dpf control and 100 nM PCB153 exposed larvae. Control ($n = 172$), 5-HTP ($n = 80$), L-DOPA ($n = 94$), haloperidol (Control $n = 178$, PCB153 $n = 81$), and bicuculline (Control $n = 160$, PCB153 $n = 173$). All data points are biologically independent samples from at least three independent experiments and mean ± SEM are shown in the plots. Significant differences to respective controls (GLM, $p < 0.01$) are indicated by open symbols. **c** Representative maximum intensity z-projection from confocal stack after photoconversions of freely swimming 6 dpf CaMPARI larvae. Scale bar = 100 μm. Ratio of red to green fluorescence intensity in the rostral hindbrain (indicated by dashed line in image) in DMSO ($n = 14$) and 1000 nM PCB153 ($n = 14$) exposed swimming larvae in 4 °C (cold) medium. Asterisks indicate significant differences to controls (two-way ANOVA, *$p = 0.0277$, ***$p = 0.0004$). All data points are biologically independent samples from two independent experiments (trials) and the horizontal lines are indicating the mean.

3-methoxytyramine hydrochloride and the inhibitory transmitter GABA were substantially increased (Fig. 5a). With dopamine playing a critical role in motor activity, we hypothesize that PCB153 impairs dopaminergic neurotransmission and subsequently increases GABA levels, leading to the predominant LLC response.

Furthermore, we propose that GABA is involved in the swelling of the afferent terminals (Fig. 3) as GABA activates Cl⁻ channels leading to an influx of Cl⁻ accompanied by H_2O[66,67]. The authors report that the osmotic neuronal swelling alters neuronal activity. This study thus provides additional evidence that GABA is involved in the neurobehavioral mode of action of higher chlorinated NDL PCBs, as has been shown for lower chlorinated congeners[68].

An important finding of this study is that PCB153-exposed larvae can execute SLC when treated with haloperidol (Fig. 5b), a D2-antagonist that can increase dopamine turnover in acute exposure[69]. This result suggests that disruption of dopamine turnover is a major mechanism involved in the sensory deficit in PCB153-treated larvae, although other factors may contribute as well. There is a large body of evidence showing that NDL PCBs, including PCB153, modulate

dopaminergic neurotransmission by inhibiting the dopamine precursor enzyme tyrosine hydroxylase and dopamine synthesis itself, in both neural crest cells and adult laboratory animal models including non-human primates[25,26,28,70]. In zebrafish larvae, PCB153 exposure during development elicited differential expression of nine genes related to the dopamine pathway, including tyrosine hydroxylase 2 (*th2*)[62]. Yet linking such effects to behavior is rare. Tanaka et al. suggested that the NDL PCB dominant mixture Aroclor 1254 and BDE-47 functionally inhibited dopaminergic neurons in early zebrafish embryos, as increased activity in 26 hpf embryos was inhibited by supplementation with L-tyrosine and L-DOPA[65].

The restoration of the delayed startle phenotype by haloperidol, together with the increased levels of a dopamine metabolite and GABA in PCB153-exposed larvae (Fig. 5), indicates that disruption of dopaminergic and GABAergic signaling between neurons of the auditory circuit is the dominant effect of PCB153-mediated aberrant motor behavior. These signaling processes are widely conserved across vertebrate species and are important in human neurological diseases. For example, a recent study found that multiple gene mutations causing defective startle response in

zebrafish were also associated with disorders of the locomotor system in humans[38].

The localization of the PCB-induced disruption of dopaminergic signal transmission is likely downstream of the hair cells, potentially in the hindbrain. Although dopaminergic neurons innervate lateral line neuromasts, where D1R antagonist reduces the hair cell activity[71], we found no difference in the hair cell activity of PCB153-exposed larvae (Fig. 3d). This is in contrast to the hindbrain, where neuronal activity was reduced in PCB153 exposed CaMPARI zebrafish larvae (Fig. 5c), indicating a reduced capacity for release or turnover of calcium. Intracellular Ca^{2+} signaling in neurons controls neurotransmitter secretion among many other cellular processes and thus may be indirectly involved in dopamine or GABA regulation. Some NDL PCBs (PCB95, PCB138) are known to inhibit voltage-gated calcium channels[29] contributing to interference with calcium homeostasis and consequently neurotransmission and synaptic plasticity[27,72–74].

The startle response in fish and amphibians is a fundamental mechanism involved in predator escape. PCB153-exposed zebrafish larvae predominantly responded with a LLC, which not only delays the response, increasing the chance to be caught by a predator but also usually does not displace the animal from its original location (Fig. 2a and ref.[47]). While survival of predator attack is likely context-dependent and species-specific, quick escape responses increase chances of survival[75], suggesting the highly abundant di-ortho-NDL PCBs may provide a substantial selection pressure and thereby could drive evolutionary adaptation. We have observed a considerable shift to LLC at concentrations of PCB153 as low as 10 nM ($3.6 \mu g L^{-1}$). PCBs are associated with sediments, where concentrations of PCB153 frequently reach multiple $\mu g kg^{-1}$[76]. PCB concentrations in organisms may be even higher due to extensive bioconcentration; killifish from New Bedford Harbor have 6.5 to 7 µg of PCB153 per g wet weight[77]. All the ortho-NDL PCBs tested in this study increased the startle latency. Thus, in the environment, where PCBs occur in mixtures of numerous congeners that likely have additive effects, the combined effect could occur at concentrations lower than that of any single congener. Taken together, these results highlight the importance of the neurotoxic potential of NDL PCBs in the natural environment.

Importantly, this study shows the lack of an effect of the potent DL PCB126 on the startle response. While in theory it is possible that higher doses of PCB126 might affect this response, it is impossible to examine this question as doses higher than we used elicit significant defects and mortality. The important conclusion is that, unlike PCB153, the PCB126 does not affect the startle response at doses like those in the environment, which are well known to cause profound changes in gene expression.

Based on the comprehensive approach presented in this study, it can be inferred that PCB153 may alter dopamine signaling and increase GABA that ultimately results in swelling of axonal terminals in the auditory circuit. The dysregulation of neurotransmitters is likely a contributing mechanism for the behavioral deficit, as GABA levels were increased and the treatment with the dopamine antagonist haloperidol restored the startle capability of PCB153-treated fish. While the involvement of connexins remains speculative, our findings provide a foothold into the dopamine dysregulating potential of PCB153 and likely other NDL PCBs in sensory-motor processing in developing vertebrates, and link that to motor behavior. In a direct comparison, the present study suggests that the adverse behavioral effects observed are induced by all NDL PCBs tested, but not by the classical DL PCB126. Whether this is true for compounds that are structurally similar to NDL PCBs, such as some PBDEs, is not known and will require further research. A key finding is that the effect of NDL PCBs on the startle latency occurs at concentrations relevant for both environmental and human exposures, thereby exposing a mechanism that is relevant to both a behavior with inherent selection pressures in fish and neurotoxicological diseases in humans. This study therewith provides valuable clues for tackling health effects in humans and wildlife caused by environmental exposure to widespread PCBs.

Methods

Animal model rationale. Zebrafish have relatively simple neural circuits, particularly for the auditory system. Many of the components of the auditory circuit are homologous in mammals and fish, including hair cells, neural transmission, and lower motorneurons, while the mechanosensory lateral line system and Mauthner cells are exclusively found in fish and a cochlea is only found in mammals. In fish, vibro-acoustic stimuli are first sensed by the hair cell bundles in the auditory, vestibular, and lateral-line systems and are rapidly encoded into trains of action potentials in the afferent neurons (Fig. 1)[78]. The signal detected through the sensory hair cells of the lateral line is transmitted through the anterior and posterior lateral line ganglia whereas the auditory input is transmitted through the VIIIth statoacoustic nerve, all of which synapse to the lateral dendrite of the Mauthner cell and two segmental homologs[79,80]. The signal is propagated down the Mauthner cell axon in the spinal cord to activate the motoneurons leading to a unilateral contraction of the trunk musculature.

Zebrafish lines and husbandry. Zebrafish (Danio rerio) were maintained at 28.5 °C and on a 12:12 h light–dark cycle according to the guidelines of the Zebrafish Model Organism Database (ZFIN, http://zfin.org) and institutional guidelines at WHOI and the experimental procedures approved by the Institutional Animal Care and Use Committee (ID Number BI21981.01). Adult zebrafish were fed brine shrimp and Gemma Micro 300 pellets (Skretting) every day. In this study, we used wild-type zebrafish of the AB strain obtained from Zebrafish International Resource Center (ZIRC), as well as several transgenic lines: the photoconvertible calcium indicator line Tg[elavl3:CaMPARI(W391F+V398L)][jf9] kindly provided by Jessica Plavicki (Brown University, USA), and the transgenic lines Tg(cntn1b:EGFP-CAAX)[81] labeling axons, Tg(olig2:EGFP)[vu12][82,83] marking oligodendrocyte precursor cell bodies, Tg(sox10:mRFP)[84] marking oligodendrocyte lineage cells, as well as Tg(mbp:EGFP-CAAX)[85] and Tg(mbp:EGFP) marking myelin sheaths (gifts from Dr. Kelly Monk, generated by Dr. Charles Kaufman in the laboratory of Dr. Leonard Zon, Harvard Medical School, Boston, MA). Zebrafish eggs were obtained by pairwise breeding and kept in 0.3x Danieau's (17 mM NaCl, 0.2 mM KCl, 0.12 mM $MgSO_4$, 0.18 mM $Ca(NO_3)_2$ and 1.5 mM HEPES, pH 7.6) in glass vials at a density of 10 individuals per 10 mL, at a constant water temperature of 28 ± 1°C and standard 14-h light/10-h dark cycle. The medium was supplemented with 1-Phenyl-2-thiourea (PTU, 0.003% w/v) from 24 hpf onwards to prevent pigment formation when necessary for imaging.

Early-life stage exposure. Fertilized eggs were used for exposures starting at 4 hpf to solvent control (0.1% DMSO, v/v), 2,2',4,4',5,5'-hexachlorobiphenyl (PCB153), 2,2',5,5'-PCB, 2,2',5,5'-tetrachlorobiphenyl (PCB52), 2,3',4,4',5-pentachlorobiphenyl (PCB118), 2,2',3,4,4',5'-hexachlorobiphenyl (PCB138), or 3,3',4,4',5-hexachlorobiphenyl (PCB126). Additionally, one exposure with PCB153 was started at 24 hpf, to assess whether effects are induced after initial neuronal cell differentiation as sensory neurons send their projection along the ectoderm as early as 16 hpf[86]. The lowest exposure concentration for PCB153 was 10 nM ($3.6 ng mL^{-1}$) in the medium, estimated to result in 14 nM (~5 $ng g^{-1}$) per lipid-rich zebrafish larva, based on comparison to PCB95 uptake levels[87]. PCB153 concentrations found in one study of maternal cord blood serum were 0.27 $ng mL^{-1}$ (0.75 nM) or 110 $ng g^{-1}$ lipid (305 nM)[8] while other reported concentrations range from 3.7 to 200 $ng g^{-1}$ lipid (10 to 554 nM)[7–10]. We also used higher exposure concentrations of PCB153 including 30 nM, 100 nM, and 1000 nM, which are found in fish of contaminated ecosystems such as the New Bedford Harbor in Massachusetts, USA[77]. For PCB52, PCB118, and PCB138, a concentration of 1000 nM was chosen, to compare to the highest concentration of PCB153. The DL PCB126 is highly cardiotoxic in the low nanomolar range and our research group has extensive experience with PCB126[88]. Based on this experience, initial experiments were performed with 1.5 nM PCB126, however, about 50% of the larvae developed cardiac edema by 6 dpf and therefore the lower concentration of 1 nM was chosen to be used in the startle response assay. The concentration of 1 nM is still highly effective at activating the aryl hydrocarbon receptor and the expression of AHR target genes. Exposures were refreshed daily until four days post-fertilization (dpf) and all larvae were kept in Danieau's from 5 to 6 dpf. All imaging and behavioral assays were performed at 6 dpf, except for the touch assay, which was performed at 26 hpf. For all behavioral assays, only larvae with an inflated swim bladder were used.

The influence of neurotransmitters on the startle behavior was assessed by exposures to compounds known to interfere with monoamines. At 6 dpf, larvae were evaluated for their startle behavior and then immersed in the dopamine precursors L-DOPA (1 mM) or L-tyrosine (1 mM), dopamine receptor agonist quinpirole (10 µM), dopamine D2-receptor antagonist and GABA receptor modulator haloperidol (10 µM), $GABA_A$ receptor antagonist bicuculline (10 µM), endogenous serotonin 5-HT (10 µM), and serotonin precursor 5-HTP (1 mM) for 30 min in the well before assessing the startle

behavior again. Additionally, the effect of neurotransmitter modulation during development on startle response was assessed by exposing larvae from 4 to 120 hpf to L-DOPA (1 mM), L-tyrosine (1 mM), and quinpirole (10 μM).

Behavioral assays. Larval locomotion was monitored using the Noldus Daniovison system (Noldus Information Technology, Leesburg, VA, USA) using 6-dpf larvae distributed in 48-well plates (1 larva per well). After an acclimation period of 40 min in the illuminated chamber, spontaneous swimming activity was tracked for 10 minutes. Following the spontaneous swimming, three alternating cycles of dark and light conditions (10 min each) were run. The experiment was repeated three times with cohorts from separate breeding events ($n = 24$ per group and breeding event). Video data were recorded with 30 frames per second via an infrared camera. Obtained data were analyzed with the supplied software EthoVision XT® 12 (Noldus. Inc.).

The activity of Rohon-Beard sensory neurons was tested at 26 hpf by lightly touching DMSO- and 1000 nM PCB153-exposed embryos ($n = 10$ per group and breeding event) using a piece of fishing line affixed to a glass pipette. Each embryo was touched ten times and the response was scored as follows: 0, no response; 0.5, light tail flicking response, 1, coiling in the opposite direction of the touch stimulus, yielding a score of a maximum of 10 per embryo. The experiment was repeated twice with cohorts from separate breeding events.

Vibro-acoustic startle response was assessed as developed by Panlilio et al.[89]. Briefly, the acoustic stimuli were delivered by a vibrational exciter producing acoustic vibrations at a frequency of 1000 Hz for a duration of 2 ms at four different amplitudes (32, 38, 41, 43 dB). For each amplitude, the stimulus was delivered four times, spaced 20 s apart, to a 4×4 well-plate mounted on top of the speaker, each well containing an individual larva. The response was tracked with a high-speed camera (Edgertronic SC1) at 1000 frames s⁻¹ for 250 ms (13 ms before and 237 ms after the stimulus). A PulsePal was used to synchronize the camera recording to the acoustic stimuli using a TTL pulse. Automated analysis of larval movement kinematics (response frequency, latency, turning angle) was performed using the FLOTE software package[42]. Each treatment group was assessed at least three times with eggs from different clutches. The total replicate numbers are stated in Supplementary Table 1.

A startle response in fish can be executed with a short latency C-bend (SLC) or long latency C-bend (LLC), with the SLC being the more frequent response at higher stimulus intensities. The cut-off time between SLC and LLC can vary depending on environmental conditions such as temperature and has been determined empirically for this experiment using a Gaussian mixture model[89] (Supplementary Fig. 12). Responses within 15 ms were categorized as SLC, latencies greater than 15 ms as LLC. Following this classification, the median response type (Relative Startle Bias) for each responsive fish was determined for each stimulus intensity (32, 38, 41, and 43 dB). Bias per individual fish was calculated as (frequency of SLC – frequency of LLC) / total responses. Pure SLC responses result in a value of +1, while pure LLC responses are a value of −1[47]. The number of replicates used in each treatment group are listed in Supplementary Table 1.

Electric field pulses (EFPs) directly activate the Mauthner cells[46]. Mauthner cell functionality was assessed by using head-restrained larvae (DMSO $n = 44$, PCB153 $n = 45$; three separate breeding events). For each run, one control and one PCB-exposed larva had their heads embedded in 1.5% agarose, side-by-side, with their tails free to move. Seven consecutive EFPs (4.4 V cm⁻¹ for 2 ms, square pulse) were applied with a recovery time of 20 s in between pulses. Response frequency, latency, and bend angle were tracked using FLOTE.

Larval growth. Larval length (from snout to the tail-fin end) was measured in DMSO ($n = 57$) and 1000 nM PCB153 ($n = 51$) exposed larvae using ImageJ. The experiment was performed three times with embryos from different clutches.

FM1-43 labeling of functional hair cells. At 6 dpf, zebrafish larvae of 1000 nM PCB153-exposed ($n = 32$) and unexposed ($n = 28$) groups were immersed in Danieau's supplemented with 3 μM FM1-43 (n-(3-triethylammoniumpropyl)-4-(4-(dibutylamino)-styryl) pyridinium dibromide; Invitrogen) for 30 s, rinsed three times in Danieau's, anesthetized in 1 mM 3-amino-benzoic acid (Tricaine), and mounted in 1.5% low melting agarose for confocal imaging of the L3 neuromast. The experiment was performed three times independently.

Visualization of Mauthner cells, kinocilia, and muscle fibers, neurons, oligodendrocyte lineage cells, and neuronal activity. Whole-mount immunohistochemistry of zebrafish larvae and brains was performed following standard procedures. Briefly, 10 AB larvae per exposure group were treated as described above and subsequently fixed in 4% paraformaldehyde (PFA) in PBS overnight at 4 °C. For labeling brain tissue, larval brains were dissected before continuing with the protocol. Multiple rinsing steps in PBS containing either 0.5% Triton-X100 or 0.1% Tween-20 (PBST) for larvae or brains, respectively, was followed by an antigen retrieval step in 150 mM Tris HCl (pH 9.0) at 70 °C[90], and a permeabilization step using proteinase K (10 μg mL⁻¹ for 3 min). Subsequently, the samples were blocked in blocking solution (10% Normal Goat Serum, 1% DMSO, 1% BSA, 88% PBST) for 1 h and then stained with blocking solution supplemented with the primary antibody for three days at 4 °C. The primary anti-neurofilament mouse monoclonal antibody 3A10 (Developmental Hybridoma Bank, antibody registry ID: AB 531874, 1:100 dilution) was used to label a subset of hindbrain spinal cord

projecting neurons such as the Mauthner cell neurons (DMSO $n = 23$, PCB153 $n = 21$). The anti-5HT rabbit polyclonal antibody (Sigma-Aldrich, #S5545, 1:500 dilution) was used to label serotonergic cells (DMSO $n = 16$, PCB153 $n = 13$). The anti-acetylated alpha-tubulin mouse polyclonal antibody (Sigma-Aldrich, #T6793, 1:1000 dilution) was used to label kinocilia and hair cell innervating neurons (DMSO $n = 26$, PCB153 $n = 24$). After several washing steps, the samples were incubated with Alexa Fluor 488- or 594-conjugated goat-anti-mouse or goat-anti-rabbit secondary antibodies (Abcam, 1:500 dilution) overnight at 4 °C and rinsed several times in PBST before mounting in ProLong Diamond Antifade mountant (Invitrogen) for imaging. For visualization of skeletal muscle fibers (DMSO $n = 20$, PCB153 $n = 20$), larvae were fixed as above, followed by permeabilization in 5% Triton-X overnight and subsequent incubation in phalloidin Alexa-546 conjugate (Invitrogen, 1:500). All staining experiments were repeated three times with larvae from independent clutches.

The *Tg(cntn1b:EGFP-CAAX)* transgenic line was used to image the cell bodies of neurons that innervate the hair cells at the L3 position in the lateral line (DMSO $n = 30$, PCB153 $n = 29$). The axons of the main caudal primary motoneurons were visualized using the *Tg(olig2:EGFP)* transgenic line (DMSO: $n = 21$, PCB153: $n = 18$). The double transgenic *Tg(olig2:EGFP) × Tg(sox10:mRFP)* was used to quantify oligodendrocyte lineage cells in the spinal cord of DMSO ($n = 22$) and 1000 nM PCB153 ($n = 16$) treated larvae[83]. The severity of myelination deficits was evaluated in *Tg(mbp:EGFP-CAAX)* larvae (DMSO $n = 26$, 1000 nM PCB153 $n = 27$) All larvae were anesthetized in tricaine (0.16% MS222) before mounting laterally in 1.5% low melting agarose on a glass-bottom microscopy dish (MatTek). Fluorescently labeled cell bodies were imaged at the distal end of the intestine, around the L3 neuromast. All experiments were performed three times independently.

Neuronal activity in DMSO- and PCB153-treated larvae was visualized using the CaMPARI (*elavl3*:CaMPARI) transgenic zebrafish line with an engineered fluorescent protein that permanently photoconverts from green to red in the presence of elevated calcium and UV light[51]. Photoconversion was achieved by mounting an LED light (405 nm; LEDSupply) between the speaker and a custom-made 3-well-plate containing the freely swimming larvae (DMSO- and PCB153-treated). Larvae of the same treatment were divided into two batches: one was photoconverted in medium at room temperature (RT) and the other one at 4 °C to elicit high neuronal activity. Photoconversion was achieved by shining the LED light for 10 s either with one vibrational stimulus of 43 dB at the start or without stimulus. Subsequently, larvae were anesthetized, embedded in agarose, and whole brains imaged using the 10x objective. The experiment was performed twice ($n = 14$ per treatment group).

Image acquisition and processing. Whole-brain, hair cells, Mauthner cell, and motor neurons were imaged on a Zeiss LSM 800 confocal system with a 10×/0.45 Plan-Apochromat, 20×/0.8 Plan-Apochromat, or 63×/1.2 C-Apochromat water immersion objective. Airy scan was applied for hair cell imaging at 63x. Z-stacks were merged to a single plane by maximal intensity projection using Fiji[91].

The number of *olig2* cells dorsal of the spinal cord was counted in confocal image stacks using the 3D projection of the Zeiss Zen blue software. Myelination was evaluated after imaging the spinal cord using the 20x objective and scored for deficits according to Panlilio et al.[89]. Representative myelination was imaged at 40x. The intensity of serotonergic neurons in the brain was measured performing a Sum Slices Z-projection followed by drawing a ROI around the 5-HT immuno-responsive cells, and per image, three random squares (area size $= 10.65 \times 10.65$) within the non-fluorescent area of the ROI for background subtraction (for orientation see Supplementary Fig. 10). Similarly, the FM1-43 intensity was measured drawing a ROI around the fluorescent hair cells and measuring the background in three random squares. Corrected total cell fluorescence (CTCF) was calculated according to the formula: Integrated density − (ROI × Mean fluorescence of background readings). CaMPARI zebrafish were mounted dorsal side oriented to the objective in 1.5 % agarose and imaged live. For quantification of active neurons in the brain of freely swimming and startling CaMPARI zebrafish larvae, Sum Slices Z-projection were analyzed for red and green fluorescence intensity in the rostral hindbrain and the ratio (F_{red}/F_{green}) calculated as previously described (Edwards et al.[92]). We define 'rostral hindbrain' as region between the rostral end of the 'cerebellar corpus' and the rostral end of the 'X vagus motorneuron cluster' (for orientation see Fig. 5c). This approach comprises a heterogenous cell population in the selected area and does not account for spatial patterns of expression. To calculate the volume of hair cell innervating neurons, automatic image thresholding with fixed minimum and maximum threshold values (30; 255, using the Otsu method) was applied to all images. Subsequently, image stacks were analyzed using an imageJ macro looping through the stack and summing the area measurements, then multiplying this sum by the depth of each slice. The presence of primary motor neurons was confirmed using the Simple Neurite Tracer plugin in Fiji. All image evaluations and quantifications were done without the knowledge of the experimental condition of the specimens.

Neurotransmitter analysis. The analysis of neurotransmitters, including histamine, L-histidine, L-glutamic acid, gamma-aminobutyric acid (GABA), acetylcholine, L-DOPA, 3-methoxytyramine, serotonin, 5-hydroxyindole-3-acetic acid, glycine, L-glutamine, L-valine, 3-hydroxytyramine and choline, was performed with a method developed in a previous study[93]. Briefly, per sample, 18 zebrafish larvae were pooled and each sample was spiked with 100 ppb isotope-labeled internal standards and then homogenized. The homogenized tissue samples were

extracted with 200 μL of 80:20 v/v ACN/Milli-Q water containing 0.1% formic acid and 1% ascorbic acid and 200 μL ACN. After protein precipitation, the supernatants were dried and redissolved in 100 μL of Milli-Q water containing 0.1% formic acid for UHPLC-MS/MS analysis. Neurotransmitters were quantified by a high-performance liquid chromatography system coupled to a Q-Exactive plus quadrupole-Orbitrap mass spectrometer (UHPLC-Q-Orbitrap, Thermo fisher, US). The separation of neurotransmitters was carried out with an Acquity UPLC HSS T3 column with Milli-Q water containing 0.1% formic acid and ACN containing 0.1% formic acid as mobile phase. The MS acquisition was performed in the full scan mode and parallel reaction monitoring mode. The experiment was performed once ($n = 4$ per treatment group).

Statistics and reproducibility. All statistical analyses were conducted using Graph Pad Prism 8.4 except some of the startle behavior analysis, which was completed in R. All quantitative data were tested for normality using the Shapiro-Wilk test, and if there were an unequal number of subjects between groups, the data were tested for homogeneity in variances using the Brown-Forsythe test. All treatment groups were compared to respective control groups. One replicate is defined as one zebrafish larva, except for the monoamine measurements where 18 larvae were pooled per sample. The sample size was based on experience from previously published experiments leading to significant results. All experiments were repeated three times with cohorts from separate breeding events except for the CaMPARI, the touch assay, and monoamine measurements.

Responsiveness to auditory stimuli (response or not) and startle type (SLC vs. LLC) was modeled in R (version 4.0.2) using a binomial generalized linear mixed effect model (glmer() from the lme4 R package)[94]. The response to electrical stimulus was modeled using glm() from the lme4 R package. For the auditory response, we included treatment as a fixed effect and the replicate experimental trials as a random effect. The model specification for fraction responding was as follows: Responders ~ TreatmentGroup + (TreatmentGroup|trial). The model specification for startle bias was as follows:
SLCorLLCresponse ~ TreatmentGroup + stimB + (1|trial). The data were analyzed fitting the model for each stimulus intensity independently. The model specification for the electrical stimulation is as follows:
Responders ~ TreatmentGroup.

To assess treatment differences of normal data with three or more groups (fluorescence intensity CaMPARI and FM1-43), two-way ANOVA comparisons were performed followed by a multiple comparison using the Tukey's correction to adjust the critical values. A Tukey-corrected p-value < 0.05 was considered statistically significant. For normal data with heterogeneity within-group variances (LLC bend angle), a Welch ANOVA followed by a Dunnett's T3 multiple comparison test was performed. For non-normal data with three or more groups (SLC bend angle), a Kruskal–Wallis followed by the Dunn's multiple comparison test was performed. For normal data with two groups (hair cell volume, number of hair cells, length, spontaneous activity, mean latency, bend angle in e-stim, oligodendrocyte lineage cell count, 5-HT intensity), an unpaired two-tailed t-test with Welch's correction (Welch's t-test) was performed. Monoamine measurements were analyzed using an unpaired t-test comparing exposed with controls. The nonparametric scoring data of the touch assay, latency in e-stim, and myelination was analyzed using a two-tailed Mann–Whitney test. The data are presented as mean ± SD with single data points (replicates) superimposed on the graph unless specified in the figure legend.

Reporting summary. Further information on research design is available in the Nature Research Reporting Summary linked to this article.

Data availability
The source data underlying the findings of this study are available within the Supplementary Data 1. Any remaining information and data such as images can be obtained from the corresponding author upon request.

References
1. Landrigan, P. J. et al. The Lancet Commission on pollution and health. *Lancet* **391**, 462–512 (2018).
2. Grandjean, P. & Landrigan, P. J. Neurobehavioural effects of developmental toxicity. *Lancet Neurol.* **13**, 330–338 (2014).
3. Boix, J., Cauli, O. & Felipo, V. Developmental exposure to polychlorinated biphenyls 52, 138 or 180 affects differentially learning or motor coordination in adult rats *mechanisms involved. Neuroscience* **167**, 994–1003 (2010).
4. Boucher, O., Muckle, G. & Bastien, C. H. Prenatal exposure to polychlorinated biphenyls: a neuropsychologic analysis. *Environ. Health Perspect.* **117**, 7–16 (2009).
5. Ennaceur, S., Gandoura, N. & Driss, M. R. Distribution of polychlorinated biphenyls and organochlorine pesticides in human breast milk from various locations in Tunisia: Levels of contamination, influencing factors, and infant risk assessment. *Environ. Res.* **108**, 86–93 (2008).
6. Lancz, K. et al. Duration of breastfeeding and serum PCB 153 concentrations in children. *Environ. Res.* **136**, 35–39 (2015).
7. Herbstman, J. B. et al. Determinants of prenatal exposure to polychlorinated biphenyls (PCBs) and polybrominated diphenyl ethers (PBDEs) in an urban population. *Environ. Health Perspect.* **115**, 1794–1800 (2007).
8. Lancz, K. et al. Ratio of cord to maternal serum PCB concentrations in relation to their congener-specific physicochemical properties. *Int J. Hyg. Env. Health* **218**, 91–98 (2015).
9. Bergonzi, R. et al. Distribution of persistent organochlorine pollutants in maternal and foetal tissues: data from an Italian polluted urban area. *Chemosphere* **76**, 747–754 (2009).
10. Patel, J. F., Hartman, T. J., Sjodin, A., Northstone, K. & Taylor, E. V. Prenatal exposure to polychlorinated biphenyls and fetal growth in British girls. *Environ. Int.* **116**, 116–121 (2018).
11. Rice, D. & Barone, S. Critical periods of vulnerability for the developing nervous system: Evidence from humans and animal models. *Environ. Health Perspect.* **108**, 511–533 (2000).
12. Trnovec, T. et al. Serum PCB concentrations and cochlear function in 12-year-old children. *Environ. Sci. Technol.* **44**, 2884–2889 (2010).
13. Jusko, T. A. et al. Prenatal and postnatal serum PCB concentrations and cochlear function in children at 45 months of age. *Environ. Health Perspect.* **122**, 1246–1252 (2014).
14. Ribas-Fitó, N., Sala, M., Kogevinas, M. & Sunyer, J. Polychlorinated biphenyls (PCBs) and neurological development in children: A systematic review. *J. Epidemiol. Community Health* **55**, 537–546 (2001).
15. Walkowiak, J. et al. Environmental exposure to polychlorinated biphenyls and quality of the home environment: effects on psychodevelopment in early childhood. *Lancet* **358**, 1602–1607 (2001).
16. Chen, Y.-C. J., Guo, Y.-L., Hsu, C.-C. & Rogan, W. J. Cognitive development of Yu-Cheng ('Oil Disease') children prenatally exposed to heat-degraded PCBs. *JAMA* **268**, 3213 (1992).
17. Berger, D. F. et al. Hyperactivity and impulsiveness in rats fed diets supplemented with either Aroclor 1248 or PCB-contaminated St. Lawrence river fish. *Behav. Brain Res.* **126**, 1–11 (2001).
18. Johansen, E. B. et al. Behavioral changes following PCB 153 exposure in the spontaneously hypertensive rat—an animal model of attention-deficit/hyperactivity disorder. *Behav. Brain Funct.* **10**, 1–19 (2014).
19. Crofton, K. M., Ding, D.-L., Padich, R., Taylor, M. & Henderson, D. Hearing loss following exposure during development to polychlorinated biphenyls: a cochlear site of action. *Hear. Res.* **144**, 196–204 (2000).
20. Goldey, E. S., Kehn, L. S., Lau, C., Rehnberg, G. L. & Crofton, K. M. Developmental exposure to polychlorinated biphenyls (Aroclor 1254) reduces circulating thyroid hormone concentrations and causes hearing deficits in rats. *Toxicol. Appl. Pharmacol.* **135**, 77–88 (1995).
21. Lilienthal, H., Korkalainen, M., Andersson, P. L. & Viluksela, M. Developmental exposure to purity-controlled polychlorinated biphenyl congeners (PCB74 and PCB95) in rats: Effects on brainstem auditory evoked potentials and catalepsy. *Toxicology* **327**, 22–31 (2015).
22. Lilienthal, H., Heikkinen, P., Andersson, P. L., van der Ven, L. T. M. & Viluksela, M. Auditory effects of developmental exposure to purity-controlled polychlorinated biphenyls (PCB52 and PCB180) in rats. *Toxicol. Sci.* **122**, 100–111 (2011).
23. Poon, E., Bandara, S. B., Allen, J. B., Sadowski, R. N. & Schantz, S. L. Developmental PCB exposure increases susceptibility to audiogenic seizures in adulthood. *Neurotoxicology* **46**, 117–124 (2015).
24. Stewart, A. M., Braubach, O., Spitsbergen, J., Gerlai, R. & Kalueff, A. V. Zebrafish models for translational neuroscience research: From tank to bedside. *Trends Neurosci.* **37**, 264–278 (2014).
25. Fonnum, F. & Mariussen, E. Mechanisms involved in the neurotoxic effects of environmental toxicants such as polychlorinated biphenyls and brominated flame retardants. *J. Neurochem.* **111**, 1327–1347 (2009).
26. Dervola, K. S. N., Johansen, E. B., Walaas, S. I. & Fonnum, F. Gender-dependent and genotype-sensitive monoaminergic changes induced by polychlorinated biphenyl 153 in the rat brain. *Neurotoxicology* **50**, 38–45 (2015).
27. Campagna, R. et al. Cerebellum Proteomics addressing the cognitive deficit of rats perinatally exposed to the food-relevant polychlorinated biphenyl 138. *Toxicol. Sci.* **123**, 170–179 (2011).
28. Enayah, S. H., Vanle, B. C., Fuortes, L. J., Doorn, J. A. & Ludewig, G. PCB95 and PCB153 change dopamine levels and turn-over in PC12 cells. *Toxicology* **394**, 93–101 (2018).
29. Langeveld, W. T., Meijer, M. & Westerink, R. H. S. Differential effects of 20 non-dioxin-like PCBs on basal and depolarization-evoked intracellular calcium levels in PC12 cells. *Toxicol. Sci.* **126**, 487–496 (2012).
30. Keil, K. P., Sethi, S. & Lein, P. J. Sex-dependent effects of 2,2′,3,5′,6-pentachlorobiphenyl on dendritic arborization of primary mouse neurons. *Toxicol. Sci.* **168**, 95–109 (2019).

31. Pruitt, D. L., Meserve, L. A. & Bingman, V. P. Reduced growth of intra- and infra-pyramidal mossy fibers is produced by continuous exposure to polychlorinated biphenyl. *Toxicology* **138**, 11–17 (1999).

32. Yang, D. et al. Developmental exposure to polychlorinated biphenyls interferes with experience-dependent dendritic plasticity and ryanodine receptor expression in weanling rats. *Environ. Health Perspect.* **117**, 426–435 (2009).

33. Lein, P. J. et al. Ontogenetic alterations in molecular and structural correlates of dendritic growth after developmental exposure to polychlorinated biphenyls. *Environ. Health Perspect.* **115**, 556–563 (2007).

34. Tropepe, V. & Sive, H. L. Can zebrafish be used as a model to study the neurodevelopmental causes of autism? Genes. *Brain Behav.* **2**, 268–281 (2003).

35. Maximino, C. & Herculano, A. M. A review of monoaminergic neuropsychopharmacology in zebrafish. *Zebrafish* **7**, 359–378 (2010).

36. Howe, K. et al. The zebrafish reference genome sequence and its relationship to the human genome. *Nature* **496**, 498–503 (2013).

37. Wolman, M. A. A. et al. A genome-wide screen identifies PAPP-AA-mediated IGFR signaling as a novel regulator of habituation learning. *Neuron* **85**, 1200–1211 (2015).

38. Meserve Id, J. H. et al. A forward genetic screen identifies Dolk as a regulator of startle magnitude through the potassium channel subunit Kv1.1. *PLoS Genet.* **17**, e1008943 (2021).

39. Voesenek, C. J., Muijres, F. T. & Van Leeuwen, J. L. Biomechanics of swimming in developing larval fish. *J. Exp. Biol.* **221**, jeb149583 (2018).

40. Roberts, A. Early functional organization of spinal neurons in developing lower vertebrates. *Brain Res. Bull.* **53**, 585–593 (2000).

41. Liu, Y. C. & Hale, M. E. Local spinal cord circuits and bilateral mauthner cell activity function together to drive alternative startle behaviors. *Curr. Biol.* **27**, 697–704 (2017).

42. Burgess, H. A. & Granato, M. Sensorimotor gating in larval zebrafish. *J. Neurosci.* **27**, 4984–4994 (2007).

43. Troconis, E. L. et al. Intensity-dependent timing and precision of startle response latency in larval zebrafish. *J. Physiol.* **595**, 265–282 (2017).

44. Smith, N. L. & Kimelman, D. Establishing the body plan: The first 24 h of zebrafish development. The Zebrafish in Biomedical Research: Biology, Husbandry, Diseases, and Research Applications, https://doi.org/10.1016/B978-0-12-812431-4.00007-5 (Elsevier, 2019).

45. Meyers, J. R. et al. Lighting up the senses: FM1-43 loading of sensory cells through nonselective ion channels. *J. Neurosci.* **23**, 4054–4065 (2003).

46. Tabor, K. M. et al. Direct activation of the Mauthner cell by electric field pulses drives ultrarapid escape responses. *J. Neurophysiol.* **112**, 834–844 (2014).

47. Jain, R. A. et al. A forward genetic screen in zebrafish identifies the G-protein-coupled receptor CaSR as a modulator of sensorimotor decision making. *Curr. Biol.* **28**, 1357–1369.e5 (2018).

48. Mariussen, E. & Fonnum, F. The effect of polychlorinated biphenyls on the high affinity uptake of the neurotransmitters, dopamine, serotonin, glutamate and GABA, into rat brain synaptosomes. *Toxicology* **159**, 11–21 (2001).

49. Wigestrand, M. B., Stenberg, M., Walaas, S. I., Fonnum, F. & Andersson, P. L. Non-dioxin-like PCBs inhibit [3H]WIN-35,428 binding to the dopamine transporter: a structure–activity relationship study. *Neurotoxicology* **39**, 18–24 (2013).

50. Oikonomou, G. et al. The serotonergic raphe promote sleep in zebrafish and mice. *Neuron* **103**, 686–701.e8 (2019).

51. Fosque, B. F. et al. Labeling of active neural circuits in vivo with designed calcium integrators. *Science* **347**, 755–760 (2015).

52. Klocke, C. & Lein, P. J. Evidence implicating non-dioxin-like congeners as the key mediators of polychlorinated biphenyl (PCB) developmental neurotoxicity. *Int. J. Mol. Sci.* **21**, 1013 (2020).

53. Puel JL, Pujol R, Ladrech S, Eybalin M. Alpha-amino-3-hydroxy-5-methyl-4-isoxazole propionic acid electrophysiological and neurotoxic effects in the guinea-pig cochlea. Neuroscience. *Nat. Rev. Neurosci.* **45**, 63–72. https://doi.org/10.1016/0306-4522(91)90103-u (1991).

54. Sebe JY, et al. Ca2+-Permeable AMPARs Mediate Glutamatergic Transmission and Excitotoxic Damage at the Hair Cell Ribbon Synapse. *J Neurosci.* **37**, 6162–6175. https://doi.org/10.1523/JNEUROSCI.3644-16.2017 (2017).

55. Coleman, M. Axon degeneration mechanisms: commonality amid diversity. *Nat. Rev. Neurosci.* **6**, 889–898 (2005).

56. Lacoste, A. M. B. et al. A convergent and essential interneuron pathway for mauthner-cell-mediated escapes. *Curr. Biol.* **25**, 1526–1534 (2015).

57. Kang, K. S., Wilson, M. R., Hayashi, T., Chang, C. C. & Trosko, J. E. Inhibition of gap junctional intercellular communication in normal human breast epithelial cells after treatment with pesticides, PCBs, and PBBs, alone or in mixtures. *Environ. Health Perspect.* **104**, 192–200 (1996).

58. Bager, Y., Lindebro, M. C., Martel, P., Chaumontet, C. & Wärngård, L. Altered function, localization and phosphorylation of gap junctions in rat liver epithelial, IAR 20, cells after treatment with PCBs or TCDD. *Environ. Toxicol. Pharmacol.* **3**, 257–266 (1997).

59. Machala, M. et al. Inhibition of gap junctional intercellular communication by noncoplanar polychlorinated biphenyls: Inhibitory potencies and screening for potential mode(s) of action. *Toxicol. Sci.* **76**, 187–195 (2003).

60. Nyffeler, J. et al. A structure–activity relationship linking non-planar PCBs to functional deficits of neural crest cells: new roles for connexins. *Arch. Toxicol.* **92**, 1225–1247 (2018).

61. Kang, K.-S., Park, J.-E., Ryu, D.-Y. & Lee, Y.-S. Effects and neuro-toxic mechanisms of 2,2',4,4',5,5'-hexachlorobiphenyl and endosulfan in neuronal stem cells. *J. Vet. Med. Sci.* **63**, 1183–1190 (2001).

62. Aluru, N., Krick, K. S., Mcdonald, A. M. & Karchner, S. I. Developmental exposure to PCB153 (2,2′,4,4′,5,5′-hexachlorobiphenyl) alters circadian rhythms and the expression of clock and metabolic genes. *Toxicol. Sci.* **173**, 41–52 (2020).

63. GEO Accession viewer. https://www.ncbi.nlm.nih.gov/geo/query/acc.cgi?acc=GSM2450663 (2017).

64. Serrano-Velez, J. L. et al. Abundance of gap junctions at glutamatergic mixed synapses in adult Mosquitofish spinal cord neurons. *Front. Neural Circuits* **8**, 66 (2014).

65. Tanaka, Y. et al. Aroclor 1254 and BDE-47 inhibit dopaminergic function manifesting as changes in locomotion behaviors in zebrafish embryos. *Chemosphere* **193**, 1207–1215 (2018).

66. Rungta, R. L. et al. The cellular mechanisms of neuronal swelling underlying cytotoxic edema. *Cell* **161**, 610–621 (2015).

67. Cesetti, T., Ciccolini, F. & Li, Y. GABA not only a neurotransmitter: osmotic regulation by GABA AR signaling. *Front Cell Neurosci.* **6**, 3 (2012).

68. Fernandes, E. C. A. et al. Potentiation of the human GABAA receptor as a novel mode of action of lower-chlorinated non-dioxin-like PCBs. *Environ. Sci. Technol.* **44**, 2864–2869 (2010).

69. Magnusson, O., Mohringe, B., Thorell, G. & Lake-Bakaar, D. M. Effects of the dopamine D2 selective receptor antagonist remoxipride on dopamine turnover in the rat brain after acute and repeated administration. *Pharmacol. Toxicol.* **60**, 368–373 (1987).

70. Seegal, R. F., Bush, B. & Shain, W. Lightly chlorinated ortho-substituted PCB congeners decrease dopamine in nonhuman primate brain and in tissue culture. *Toxicol. Appl. Pharmacol.* **106**, 136–144 (1990).

71. Toro, C. et al. Dopamine modulates the activity of sensory hair cells. *J. Neurosci.* **35**, 16494–16503 (2015).

72. Gafni, J., Wong, P. W. & Pessah, I. N. Non-coplanar 2,2',3,5',6-pentachlorobiphenyl (PCB 95) amplifies ionotropic glutamate receptor signaling in embryonic cerebellar granule neurons by a mechanism involving ryanodine receptors. *Toxicol. Sci.* **77**, 72–82 (2003).

73. Ta, T. A., Feng, W., Molinski, T. F. & Pessah, I. N. Hydroxylated xestospongins block inositol-1,4,5-trisphosphate-induced Ca2+ release and sensitize Ca2+-induced Ca2+ release mediated by ryanodine receptors. *Mol. Pharmacol.* **69**, 532–538 (2006).

74. Brunelli, L. et al. Insight into the neuroproteomics effects of the food-contaminant non-dioxin like polychlorinated biphenyls. *J. Proteomics.* **75**, 2417–2430 (2012).

75. McCormick, M. I., Fakan, E. & Allan, B. J. M. Behavioural measures determine survivorship within the hierarchy of whole-organism phenotypic traits. *Funct. Ecol.* **32**, 958–969 (2018).

76. Lai, Z. et al. Residual distribution and risk assessment of polychlorinated biphenyls in surface sediments of the Pearl River Delta, South China. *Bull. Environ. Contam. Toxicol.* **95**, 37–44 (2015).

77. Gräns, J. et al. Regulation of pregnane-X-receptor, CYP3A and P-glycoprotein genes in the PCB-resistant killifish (Fundulus heteroclitus) population from New Bedford Harbor. *Aquat. Toxicol.* **159**, 198–207 (2015).

78. Hudspeth, A. The cellular basis of hearing: the biophysics of hair cells. *Science* **230**, 745–752 (1985).

79. Nakayama, H. Common sensory inputs and differential excitability of segmentally homologous reticulospinal neurons in the hindbrain. *J. Neurosci.* **24**, 3199–3209 (2004).

80. Pujol-Martí, J. & López-Schier, H. Developmental and architectural principles of the lateral-line neural map. *Front. Neural Circuits* **7**, 47 (2013).

81. Panlilio, J. M., Jones, I. T., Salanga, M. C., Aluru, N. & Hahn, M. E. Developmental exposure to domoic acid disrupts startle response behavior and circuitry in zebrafish. *Toxicol. Sci.* **182**, 310–326 (2021).

82. Park, H.-C., Shin, J., Roberts, R. K. & Appel, B. An olig2 reporter gene marks oligodendrocyte precursors in the postembryonic spinal cord of zebrafish. *Dev. Dyn.* **236**, 3402–3407 (2007).

83. Shin, J., Park, H.-C., Topczewska, J. M., Mawdsley, D. J. & Appel, B. Neural cell fate analysis in zebrafish using *olig2* BAC transgenics. *Methods Cell Sci.* **25**, 7–14 (2003).

84. Takada, N., Kucenas, S. & Appel, B. Sox10 is necessary for oligodendrocyte survival following axon wrapping. *Glia* **58**, 996–1006 (2010).

85. Almeida, R. G., Czopka, T., Ffrench-Constant, C. & Lyons, D. A. Individual axons regulate the myelinating potential of single oligodendrocytes in vivo. *Development* **138**, 4443–4450 (2011).

86. Kimmel, C. B. Patterning the brain of the zebrafish embryo. *Annu. Rev. Neurosci.* **16**, 707–732 (1993).

87. Ranasinghe, P. et al. Embryonic exposure to 2,2′,3,5′,6-pentachlorobiphenyl (PCB-95) causes developmental malformations in zebrafish. *Environ. Toxicol. Chem.* **39**, 162–170 (2019).

88. Jönsson, M. E., Kubota, A., Timme-Laragy, A. R., Woodin, B. & Stegeman, J. J. Ahr2-dependence of PCB126 effects on the swim bladder in relation to expression of CYP1 and cox-2 genes in developing zebrafish. *Toxicol. Appl. Pharmacol.* **265**, 166–174 (2012).

89. Panlilio, J. M., Aluru, N. & Hahn, M. E. Developmental neurotoxicity of the harmful algal bloom toxin domoic acid: Cellular and molecular mechanisms underlying altered behavior in the zebrafish model. *Environ. Health Perspect.* **128**, 117002 (2020).

90. Inoue, D. & Wittbrodt, J. One for all-a highly efficient and versatile method for fluorescent immunostaining in fish embryos. *PLoS One* **6**, 1–7 (2011).

91. Schindelin, J. et al. Fiji: An open-source platform for biological-image analysis. *Nat. Methods* **9**, 676–682 (2012).

92. Edwards KA, Hoppa MB, Bosco G. The Photoconvertible Fluorescent Probe, CaMPARI, Labels Active Neurons in Freely-Moving Intact Adult Fruit Flies. *Front Neural Circuits.* **14**, 22 https://doi.org/10.3389/fncir.2020.00022. (2020).

93. Zhao, Y. et al. Rare earth elements lanthanum and praseodymium adversely affect neural and cardiovascular development in zebrafish (Danio rerio). *Environ. Sci. Technol.* https://doi.org/10.1021/acs.est.0c06632 (2020).

94. Bates, D., Mächler, M., Bolker, B. & Walker, S. Fitting linear mixed-effects models using lme4. *J. Stat. Softw.* **67**, 1–48 (2015).

Acknowledgements

Author contributions

N.R.B., J.M.P., J.J.S., and J.V.G. conceptualized the study, and acquired the principal funding. N.R.B., J.M.P., K.Z., Y.Z., and E.I. created methods and performed investiga-tions. J.M.P. wrote the software scripts. N.R.B. and J.M.P. conducted the formal analysis. N.R.B. created the visualizations and wrote the original draft. N.R.B., J.M.P., K.Z., Y.Z., J.J.S., and J.V.G. revised and edited the manuscript. J.J.S. and J.V.G. provided the project administration. All authors read and approved the final manuscript.

Competing interests

The authors declare no competing interests.

Additional information

Supplementary information The online version contains supplementary material available at https://doi.org/10.1038/s42003-021-02626-9.

Correspondence and requests for materials should be addressed to Nadja R. Brun, John J. Stegeman or Jared V. Goldstone.

Peer review information *Communications Biology* thanks Gilda Stefanelli and the other, anonymous, reviewers for their contribution to the peer review of this work. Primary Handling Editors: Patrick Murphy and George Inglis.

Reprints and permission information is available at http://www.nature.com/reprints

Publisher's note Springer Nature remains neutral with regard to jurisdictional claims in published maps and institutional affiliations.